Supplementary Information (SI) for ChemComm.

Supporting Information

Multichannel Afterglow Regulated by Protonation-Induced Reversed Intersystem Crossing

Ruijian Yan, Bingbing Ding, Tao Li, Chenjia Yin and Xiang Ma**

Key Laboratory for Advanced Materials and Feringa Nobel Prize Scientist Joint Research Center, Frontiers Science Center for Materiobiology and Dynamic Chemistry, Institute of Fine Chemicals, School of Chemistry and Molecular Engineering, East China University of Science and Technology, Meilong Road 130, Shanghai 200237, P. R. China
E-mail: maxiang@ecust.edu.cn

Experimental Procedures

Materials:

The compounds acridin-9(10H)-one, 1-bromo-4-fluorobenzene, 1-bromo-4-methoxybenzene, 1-bromo-4-(trifluoromethyl)benzene, N,N'-dimethylformamide(DMF), 2,2,6,6-tetramethyl-3,5-heptanedione, K_2CO_3 and CuI were purchased from commercial source without further purification before use.

General:

^{1}H NMR and ^{13}C NMR spectra were measured on a Bruker AV-400 spectrometer. The electronic spray ionization (ESI) high-resolution mass spectra were tested on a Waters LCT Premier XE spectrometer. Thermogravimetric analysis (TGA) spectra were obtained on a TGA 8000 (PerkinElmer, USA). The UV-Vis absorption spectra were obtained on a Cary 60 (Agilent Technologies) spectrophotometer. Phosphorescence and lifetime of delayed emission spectra were recorded on an Agilent Cary Eclipse spectrophotometer. Phosphorescence mode; Delay time = 0.1 ms; Gate time = 2.0 ms. Absolute PL quantum yields were determined with a spectrometer C11347-11 (Hamamatsu, Japan). Power X-ray diffraction experiments were carried out on Bruker D8 Venture diffractometer with a PHOTON 100 CMOS area detector.

1. Synthesis and characterization

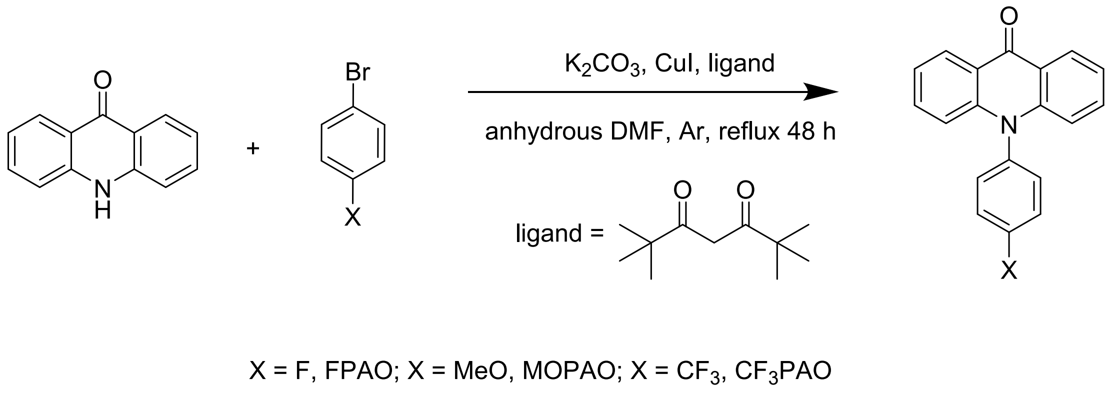

Scheme 1. Synthetic routes of FPAO, MOPAO and CF_3PAO molecules.

General procedure for the synthesis of XPAO. To the solution of acridin-9(10H)-one (976 mg, 5 mmol, 1 e.q.) and 1-bromo-4-fluorobenzene or 1-bromo-4-methoxybenzene or 1-bromo-4-(trifluoromethyl)benzene (5.5 mmol, 1.1 e.q.) in anhydrous DMF (30 ml), K_2CO_3 (760 mg, 5.5 mmol, 1.1 e.q.), CuI (96 mg, 0.5 mmol, 0.1 e.q.) and 2,2,6,6-tetramethyl-3,5-heptanedione (185 mg, 1 mmol, 0.2 e.q.) were added into the two-necked round flask. The mixture was degassed and refluxed under argon atmosphere for 48 h. After complishment of the reaction, the mixture was allowed to cool down to room temperature. Plenty of water was added to the mixture to quench the reaction and a large amount of solid was precipitated. The mixture was filtrated and the filter cake was washed with plenty of water to remove DMF. After dring in an oven, the crude procudt was purified by the column chromatography on silica gel with PE / EA = 4/1 as eluent. After that, the solid was recrystalized with EtOH to give compound FPAO (0.867 g, 60%), MOPAO (1.10 g, 73%) and CF_3PAO (1.07 g, 63%). All of theses compounds were identified as yellow crystaline solid.

10-(4-fluorophenyl)acridin-9(10H)-one (FPAO). ^1H NMR (400 MHz, DMSO-d_6) δ 8.38 (dd, J = 8.1, 1.7 Hz, 2H), 7.71 – 7.60 (m, 6H), 7.34 (td, J = 8.0, 7.0, 1.0 Hz, 2H), 6.76 (d, J = 8.6 Hz, 2H). ^{13}C NMR (101 MHz, Chloroform-d) δ 178.12, 162.87 (d, J = 251.5 Hz), 143.17, 134.85 (d, J = 3.0 Hz), 133.42, 131.98 (d, J = 9.1 Hz), 127.40, 121.86, 121.71, 118.25 (d, J = 22.2 Hz), 116.58. HRMS (DART) (m/z): $[M+H]^+$ cacl. for $[C_{19}H_{13}FNO]^+$, 290.0976; found, 290.0963.

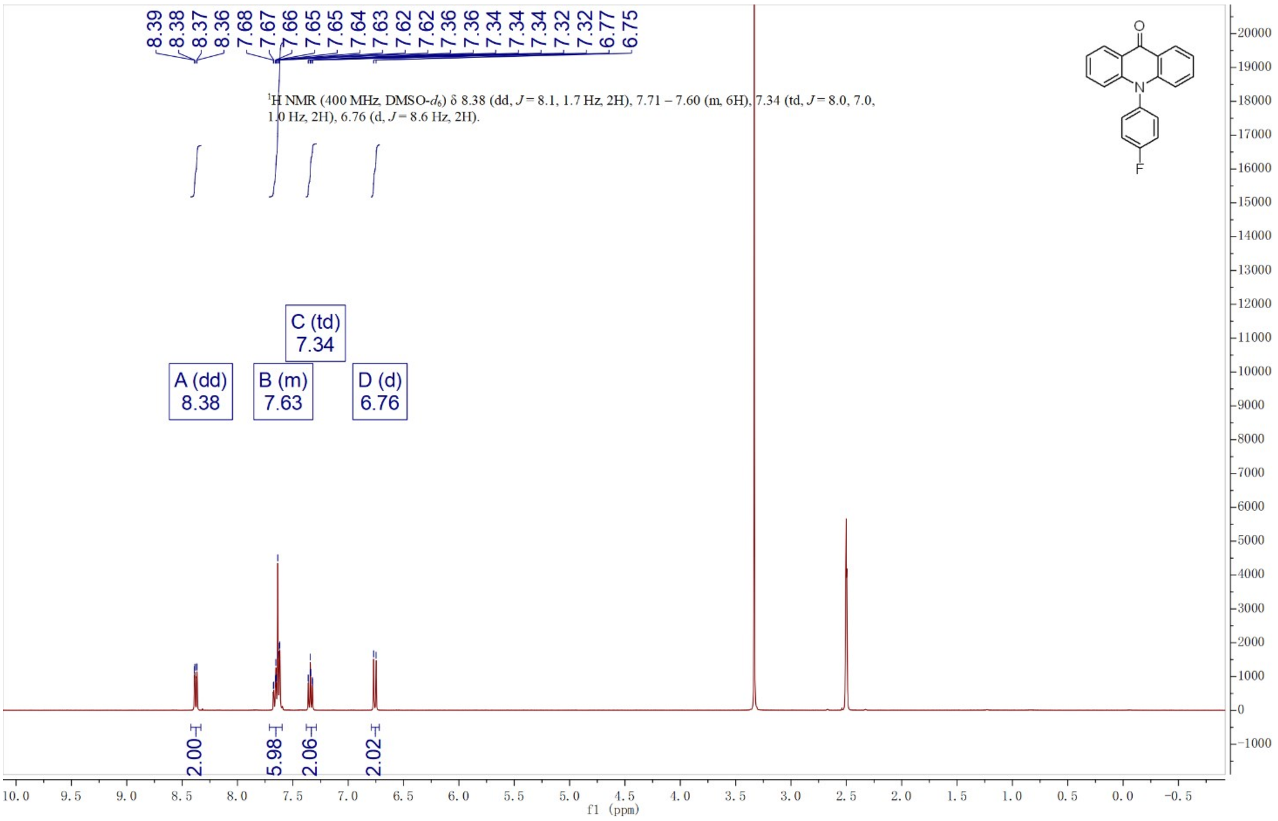

Figure S1. ^1H NMR spectra of FPAO.

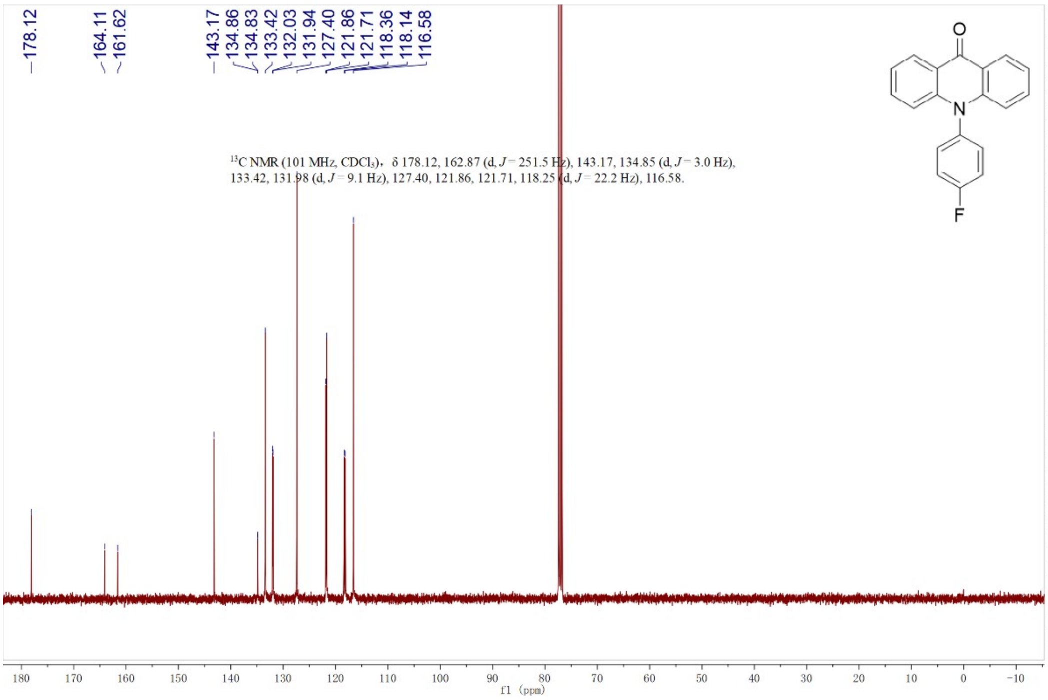

^{13}C NMR (101 MHz, CDCl$_3$)， δ 178.12, 162.87 (d, *J* = 251.5 Hz), 143.17, 134.85 (d, *J* = 3.0 Hz), 133.42, 131.98 (d, *J* = 9.1 Hz), 127.40, 121.86, 121.71, 118.25 (d, *J* = 22.2 Hz), 116.58.

Figure S2. ^{13}C NMR spectra of FPAO.

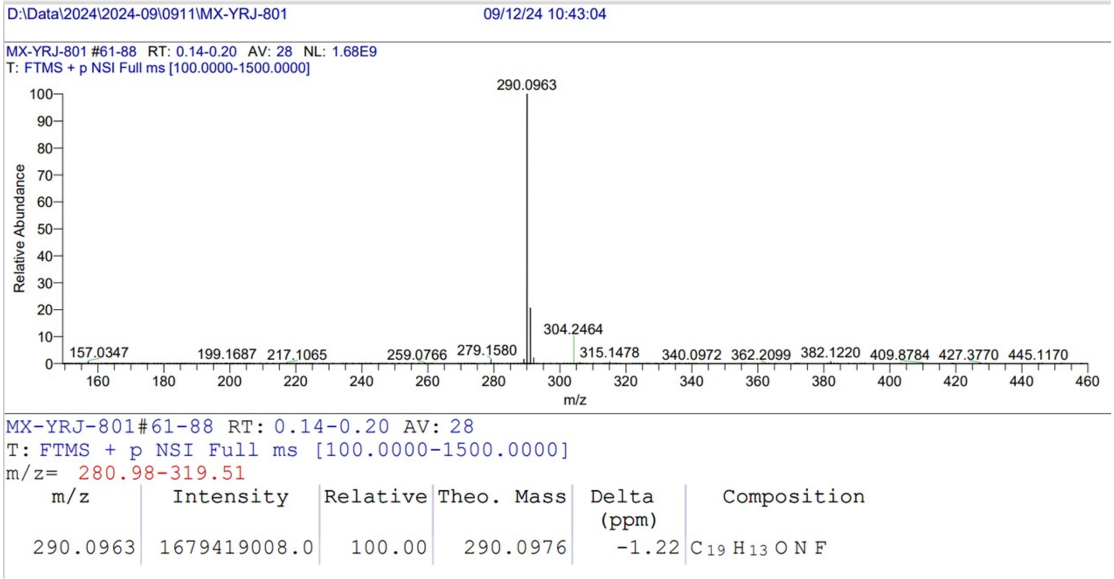

D:\Data\2024\2024-09\0911\MX-YRJ-801 09/12/24 10:43:04

MX-YRJ-801 #61-88 RT: 0.14-0.20 AV: 28 NL: 1.68E9
T: FTMS + p NSI Full ms [100.0000-1500.0000]

```
MX-YRJ-801#61-88 RT: 0.14-0.20 AV: 28
T: FTMS + p NSI Full ms [100.0000-1500.0000]
m/z= 280.98-319.51
     m/z        Intensity     Relative Theo. Mass  Delta       Composition
                                                   (ppm)
  290.0963   1679419008.0    100.00    290.0976    -1.22  C19 H13 O N F
```

Figure S3. HRMS spectra of FPAO.

10-(4-methoxyphenyl)acridin-9(10H)-one (MOPAO). ^{1}H NMR (400 MHz, DMSO-d_6) δ 8.37 (dd, *J* = 8.0, 1.6 Hz, 2H), 7.64 (ddd, *J* = 8.7, 7.0, 1.7 Hz, 2H), 7.50 – 7.41 (m, 2H), 7.37 – 7.25 (m, 4H), 6.80 (d, *J* = 8.6 Hz, 2H), 3.91 (s, 3H). ^{13}C NMR (101 MHz, Chloroform-*d*) δ 178.22, 160.14, 143.51, 133.26, 131.36, 131.00, 127.26, 121.85, 121.48, 116.92, 116.18, 55.72. HRMS (DART) (m/z): [M+H]$^+$ cacl. for [$C_{20}H_{16}NO_2$]$^+$, 302.1176; found, 302.1163.

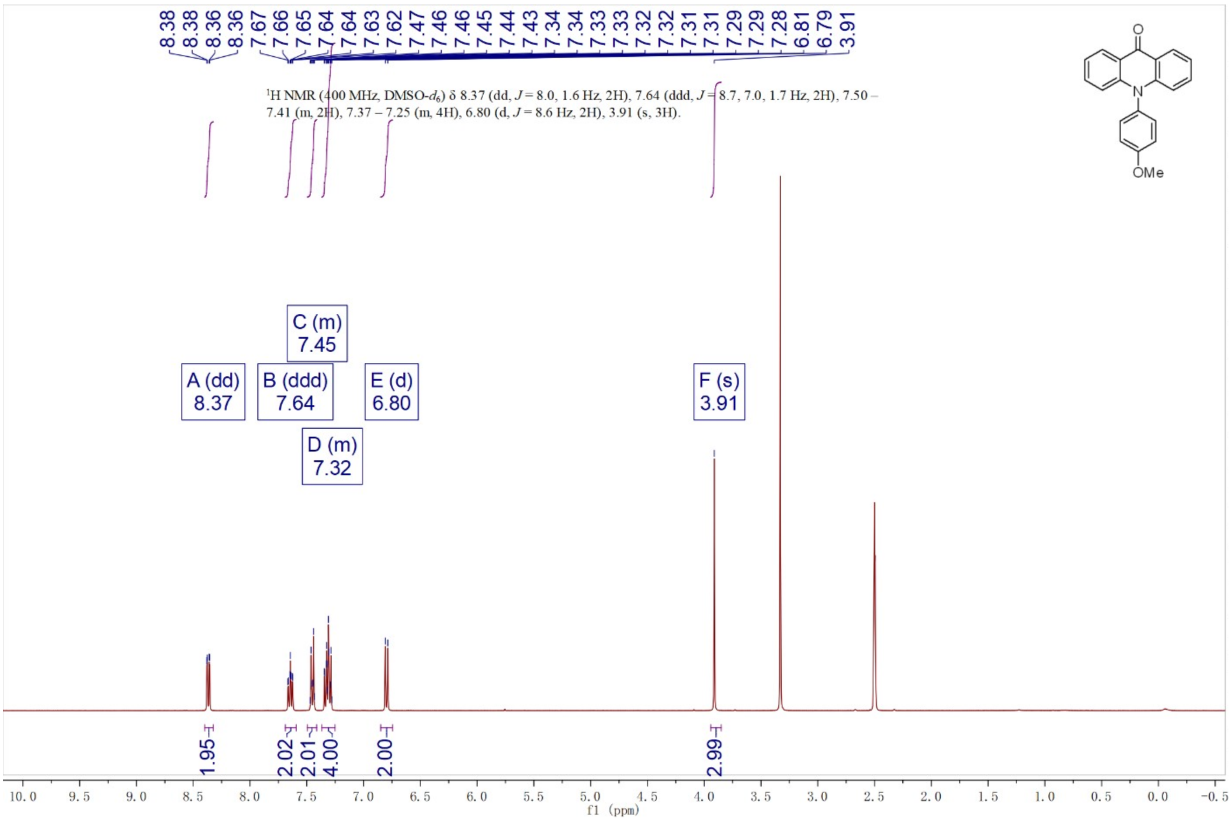

^{1}H NMR (400 MHz, DMSO-d_6) δ 8.37 (dd, J = 8.0, 1.6 Hz, 2H), 7.64 (ddd, J = 8.7, 7.0, 1.7 Hz, 2H), 7.50 – 7.41 (m, 2H), 7.37 – 7.25 (m, 4H), 6.80 (d, J = 8.6 Hz, 2H), 3.91 (s, 3H).

Figure S4. ^{1}H NMR spectra of MOPAO.

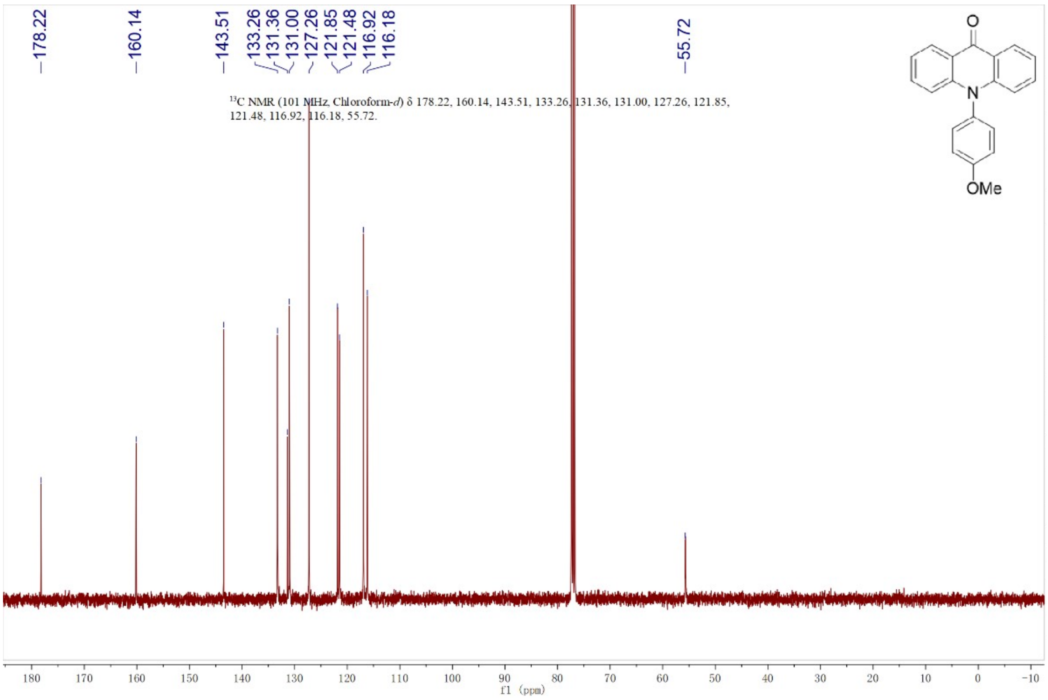

^{13}C NMR (101 MHz, Chloroform-d) δ 178.22, 160.14, 143.51, 133.26, 131.36, 131.00, 127.26, 121.85, 121.48, 116.92, 116.18, 55.72.

Figure S5. ^{13}C NMR spectra of MOPAO.

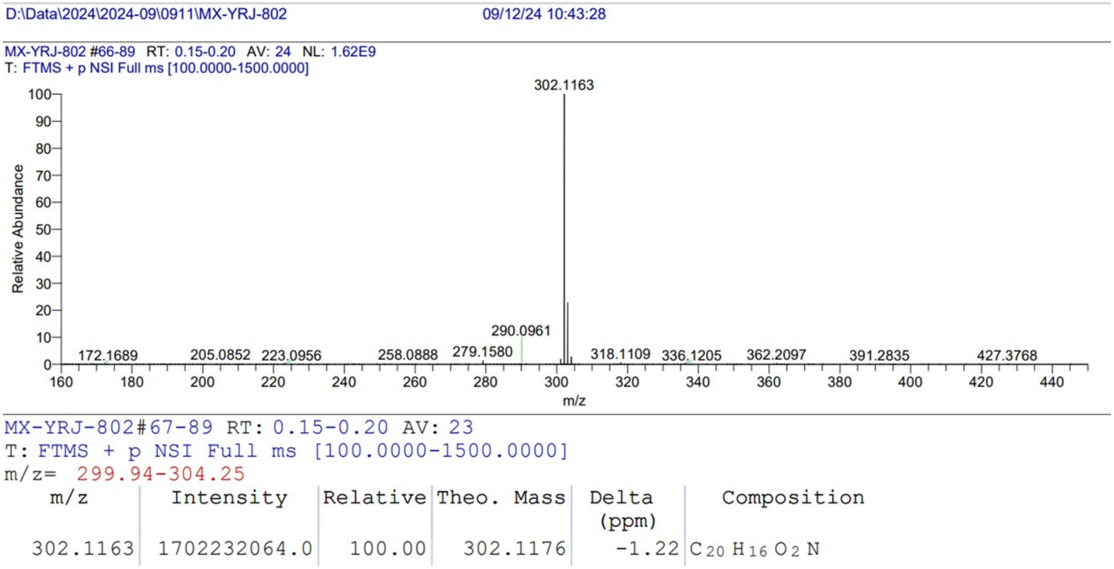

```
MX-YRJ-802#67-89 RT: 0.15-0.20 AV: 23
T: FTMS + p NSI Full ms [100.0000-1500.0000]
m/z= 299.94-304.25
    m/z    | Intensity    |Relative|Theo. Mass| Delta  |   Composition
           |              |        |          | (ppm)  |
  302.1163 | 1702232064.0 | 100.00 | 302.1176 |  -1.22 |C20 H16 O2 N
```

Figure S6. HRMS spectra of MOPAO.

10-(4-(trifluoromethyl)phenyl)acridin-9(10H)-one (CF_3PAO). ^1H NMR (400 MHz, DMSO-d_6) δ 8.39 (dd, *J* = 8.0, 1.7 Hz, 2H), 8.17 (d, *J* = 8.3 Hz, 2H), 7.85 (d, *J* = 8.1 Hz, 2H), 7.65 (td, *J* = 8.7, 7.0, 1.7 Hz, 2H), 7.36 (td, *J* = 8.1, 7.0, 1.0 Hz, 2H), 6.71 (d, *J* = 8.6 Hz, 2H).^{13}C NMR (101 MHz, Chloroform-*d*) δ 178.05, 142.70, 142.30, 133.56, 131.96 (q, *J* = 33.3 Hz), 131.03, 128.40 (q, *J* = 3.03 Hz), 127.55, 124.6 (q, *J* = 272.7 Hz), 121.95, 121.87, 116.34. HRMS (DART) (m/z): $[M+H]^+$ cacl. for $[C_{20}H_{16}NO_2]^+$, 340.0944; found, 340.0922.

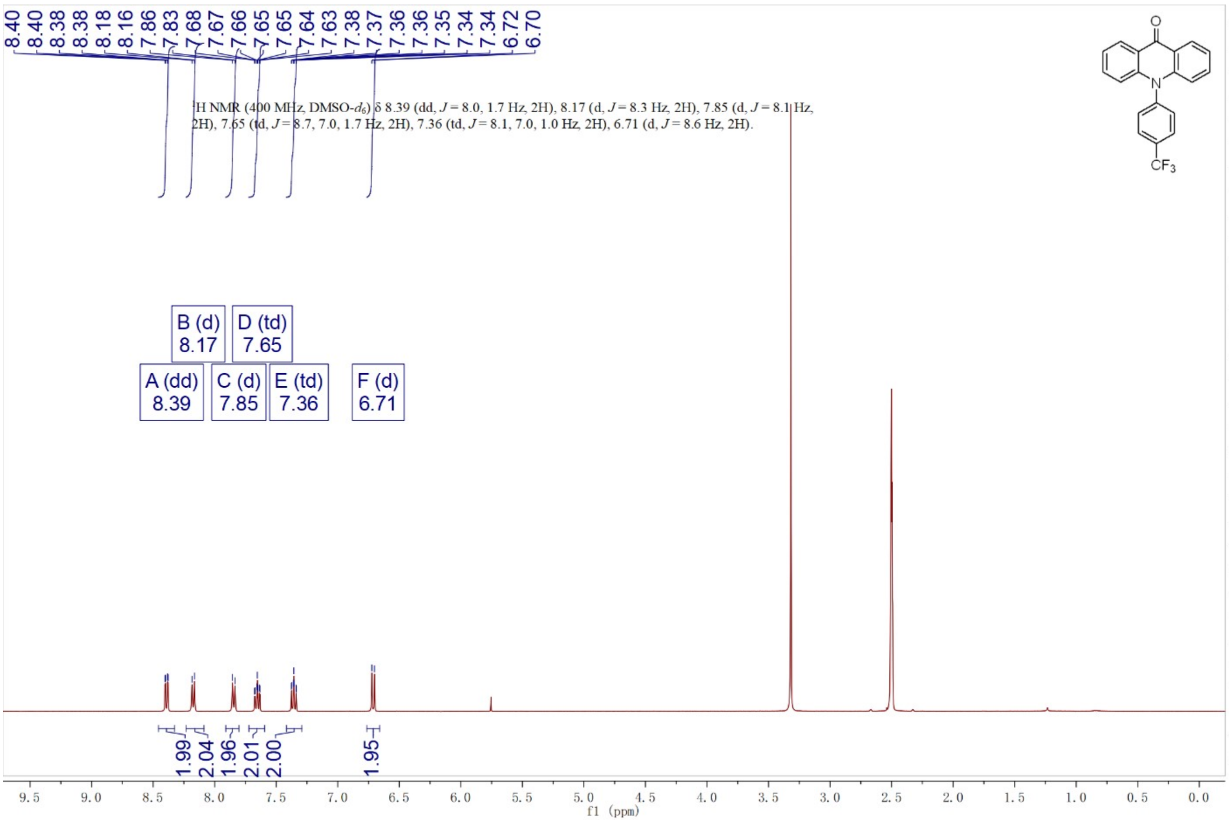

^{1}H NMR (400 MHz, DMSO-d_6) δ 8.39 (dd, J = 8.0, 1.7 Hz, 2H), 8.17 (d, J = 8.3 Hz, 2H), 7.85 (d, J = 8.1 Hz, 2H), 7.65 (td, J = 8.7, 7.0, 1.7 Hz, 2H), 7.36 (td, J = 8.1, 7.0, 1.0 Hz, 2H), 6.71 (d, J = 8.6 Hz, 2H).

Figure S7. ^{1}H NMR spectra of CF_3PAO.

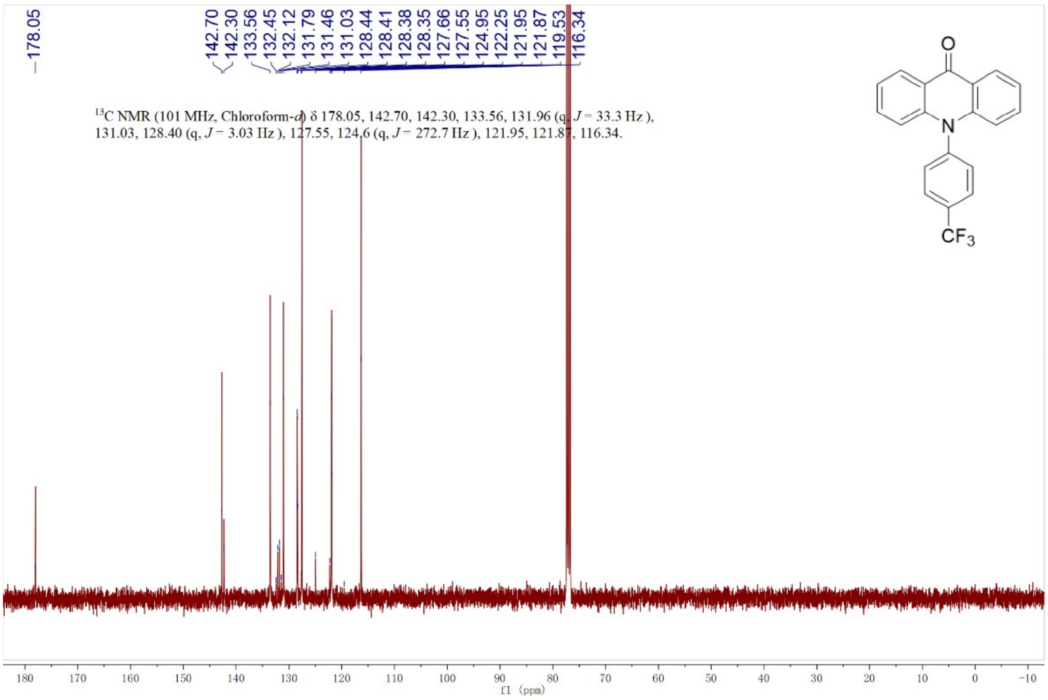

^{13}C NMR (101 MHz, Chloroform-d) δ 178.05, 142.70, 142.30, 133.56, 131.96 (q, J = 33.3 Hz), 131.03, 128.40 (q, J = 3.03 Hz), 127.55, 124.6 (q, J = 272.7 Hz), 121.95, 121.87, 116.34.

Figure S8. ^{13}C NMR spectra of CF_3PAO.

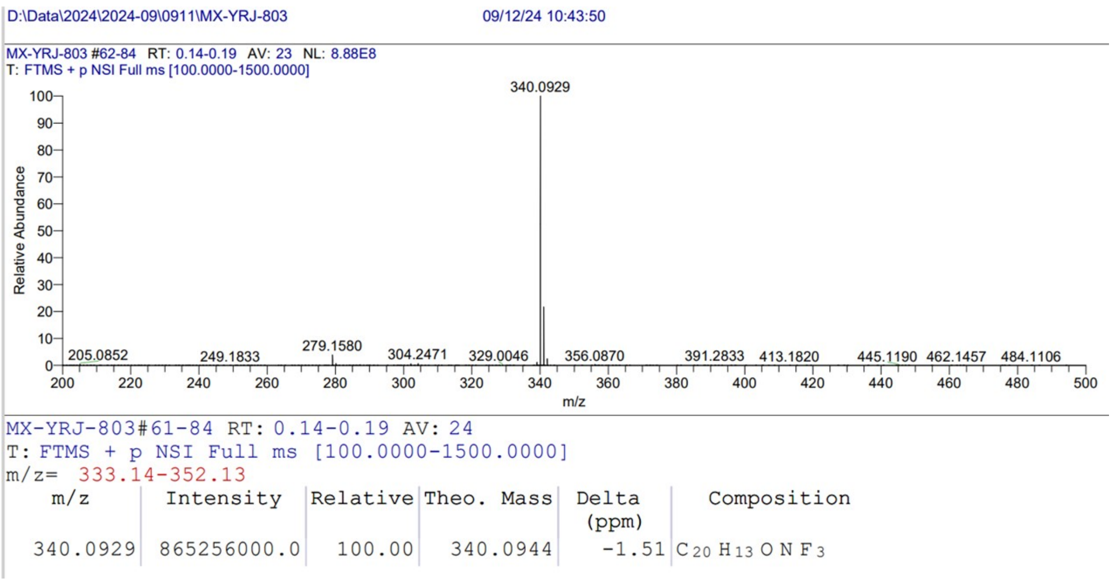

```
D:\Data\2024\2024-09\0911\MX-YRJ-803                    09/12/24 10:43:50

MX-YRJ-803 #62-84  RT: 0.14-0.19  AV: 23  NL: 8.88E8
T: FTMS + p NSI Full ms [100.0000-1500.0000]
```

```
MX-YRJ-803#61-84 RT: 0.14-0.19 AV: 24
T: FTMS + p NSI Full ms [100.0000-1500.0000]
m/z=  333.14-352.13
     m/z     |  Intensity    |Relative |Theo. Mass |  Delta    |    Composition
             |               |         |           |  (ppm)    |
  340.0929   |  865256000.0  |  100.00 |  340.0944 |    -1.51  |C 20 H 13 O N F 3
```

Figure S9. HRMS spectra of CF_3PAO.

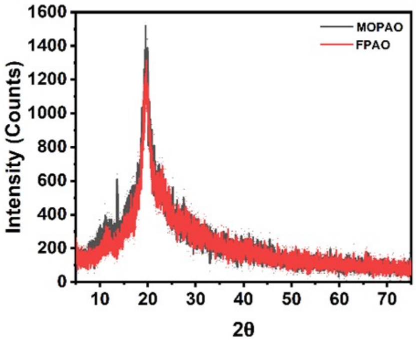

Figure S10. The XRD spectra of the MOPAO@PVA and FPAO@PVA films.

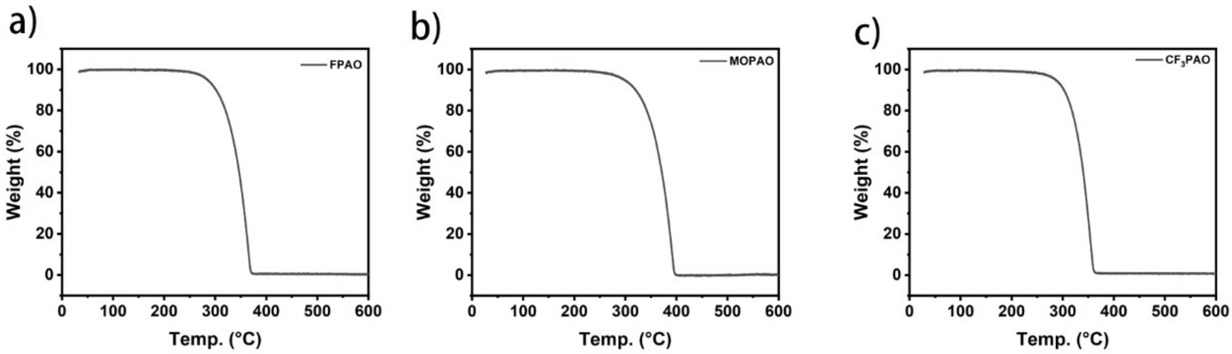

Figure S11. The TGA spectra of a) FPAO, b) MOPAO and c) CF_3PAO powder.

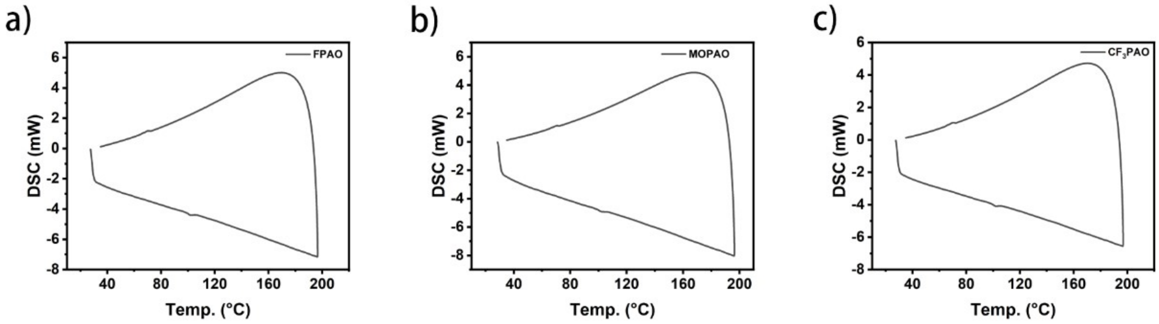

Figure S12. The DSC spectra of a) FPAO, b) MOPAO and c) CF_3PAO powder.

2. Photophysical data

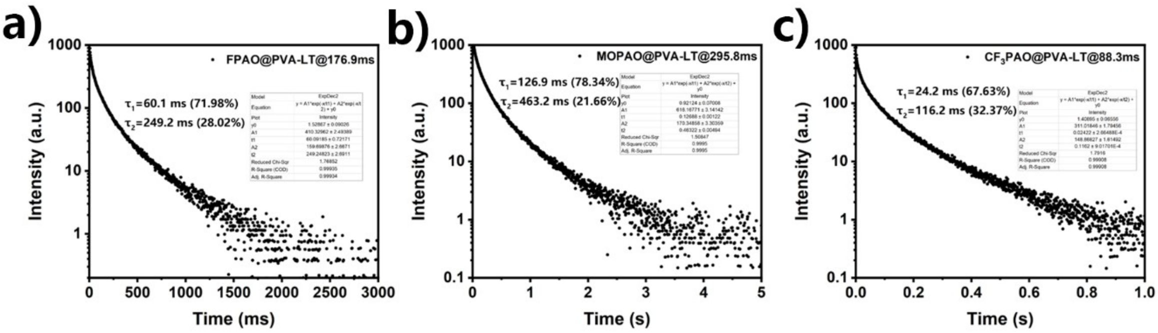

Figure S13. The fitted TADF lifetime curves of FPAO@PVA, MOPAO@PVA and CF3PAO@PVA films.

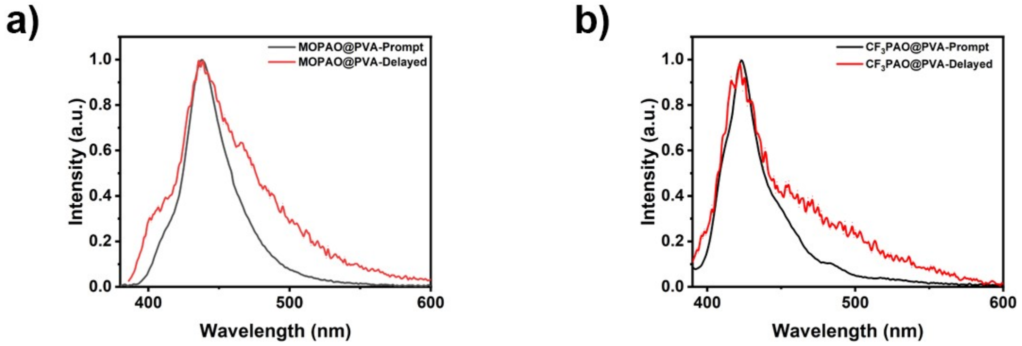

Figure S14. The prompt and delayed spectra of a) MOPAO@PVA and b) CF_3PAO@PVA.

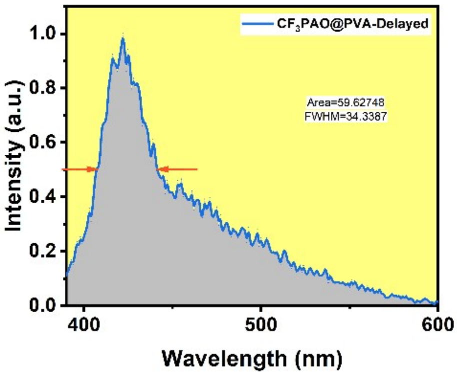

Figure S15. The calculated FWHM value of $CF_3PAO@PVA$.

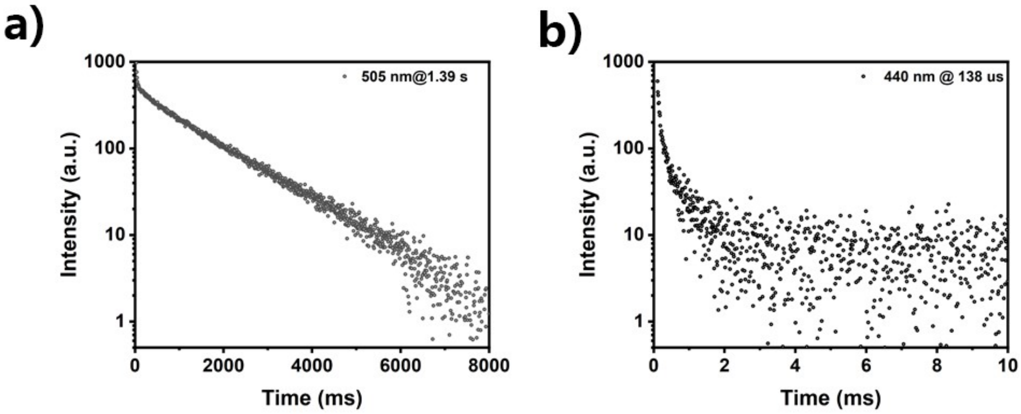

Figure S16. The emission decay spectra of FPAO@PVA film at a) 505 nm and b) 440 nm under 80 K.

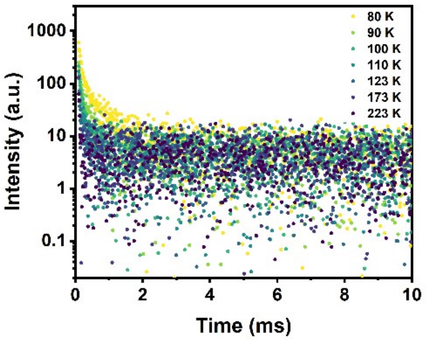

Figure S17. Temperature-dependent emission decay spectra of FPAO@PVA film at 440 nm.

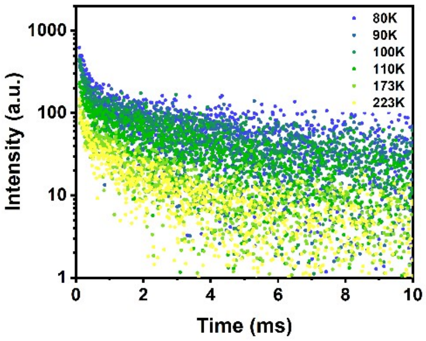

Figure S18. Temperature-dependent emission decay spectra of FPAO microcrystal at 545 nm.

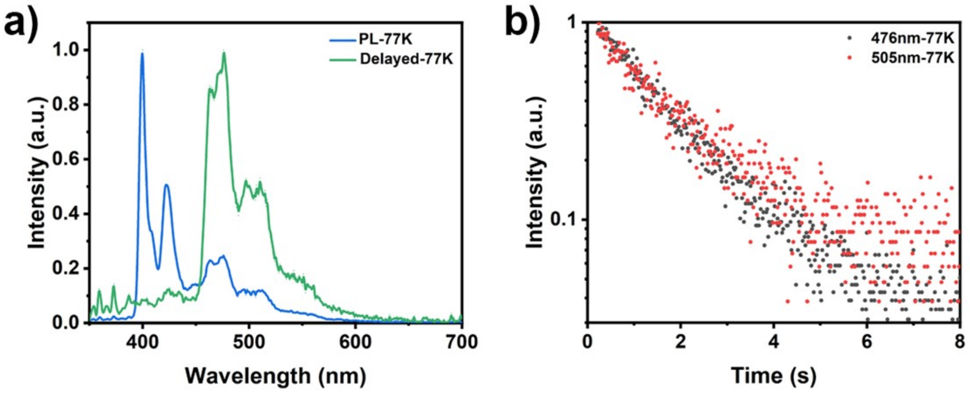

Figure S19. a) The steady PL and delayed PL spectra and b) normalized emission decay spectra at 476 nm and 505 nm ($\lambda_{ex} = 250$ nm) of FPAO in 2-MeTHF (10^{-5} M) under 77 K.

ΔE_{ST} was calculated based on the following formula:

$$\Delta E_{ST} = hc\left|\frac{\lambda_2 - \lambda_1}{\lambda_2\lambda_1}\right|$$

Here, c represents the speed of light in vacuum, h is the Planck's constant, and λ_1 and λ_2 are the peak wavelength of fluorescence and phosphorescence emission spectra, respectively. By substituting the correct wavelength into the formula, the value of ΔE_{ST} is calculated.[1]

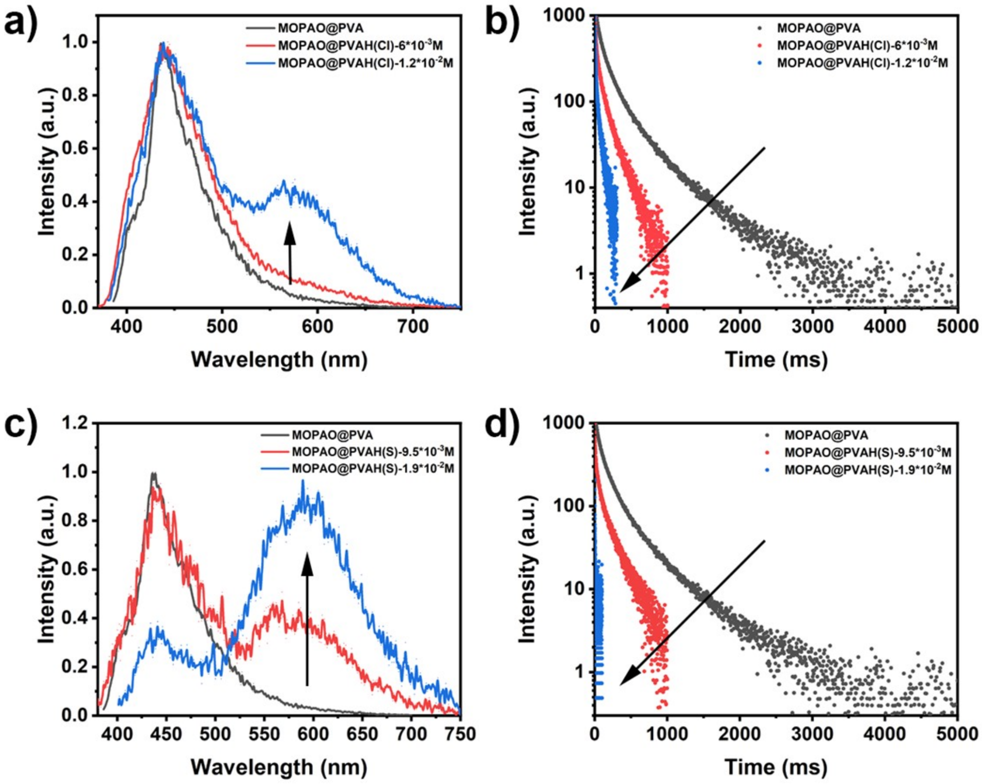

Figure S20. a) The normalized delayed emission and b) emission decay spectra at around 440 nm of MOPAO@PVAH (Cl) with varied hydrochloric acid content; c) The normalized delayed emission and d) emission decay spectra at around 440 nm of MOPAO@PVAH (S) with varied sulfuric acid content.

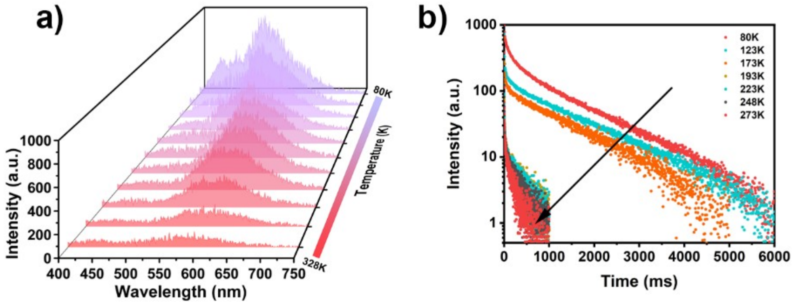

Figure S21. Temperature-dependent spectra of MOPAO@PVAH. a) Delayed emission spectra from 80 to 328 K ; b) Lifetime decay spectra at around 590 nm from 80 to 273 K.

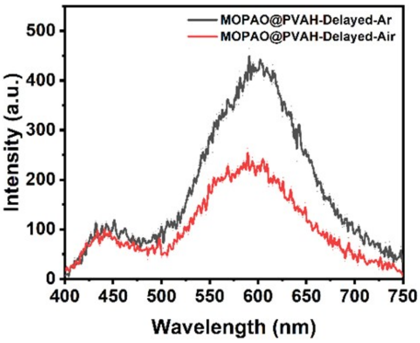

Figure S22. The delayed emission spectra of MOPAO@PVAH film in Ar and Air atmosphere.

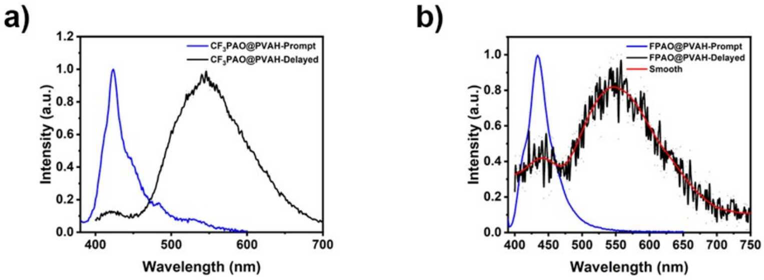

Figure S23. The prompt and delayed emission spectra of a) CF_3PAO@PVAH and b) FPAO@PVAH.

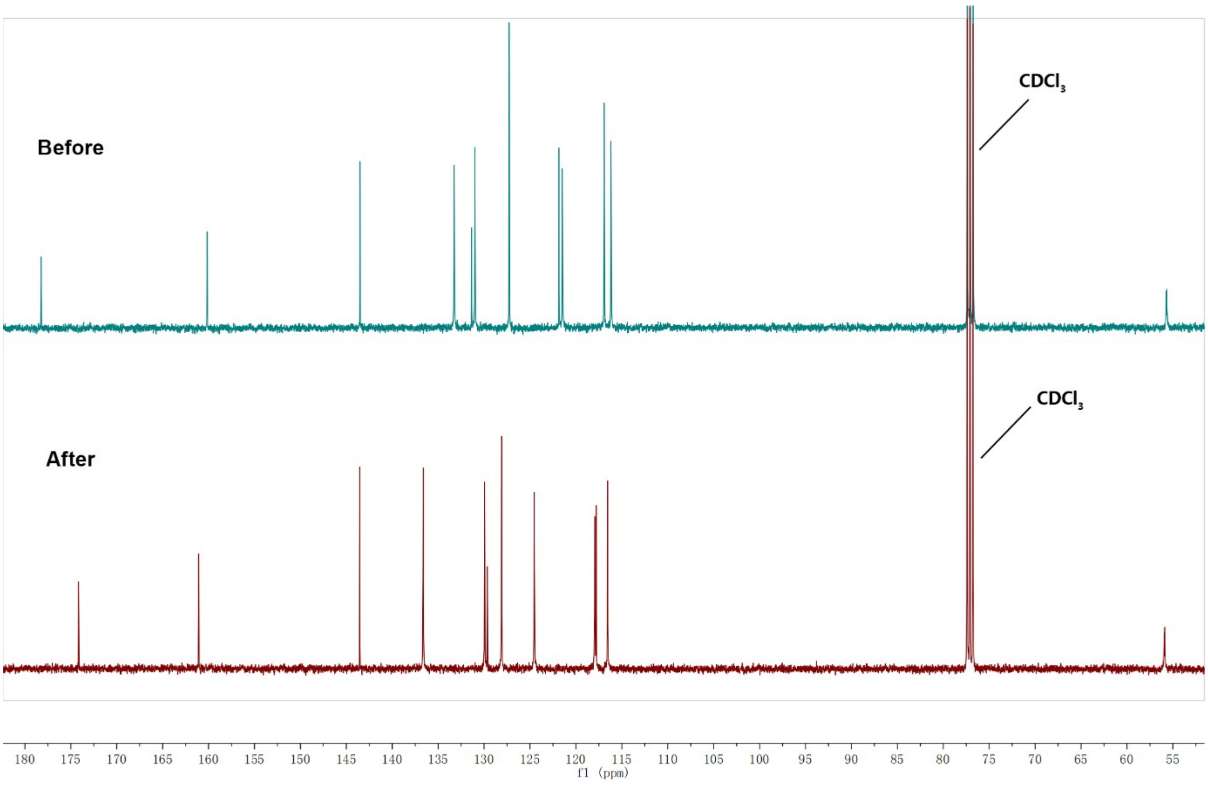

Figure S24. ^{13}C NMR spectra ($CDCl_3$) of MOPAO before and after acid addition.

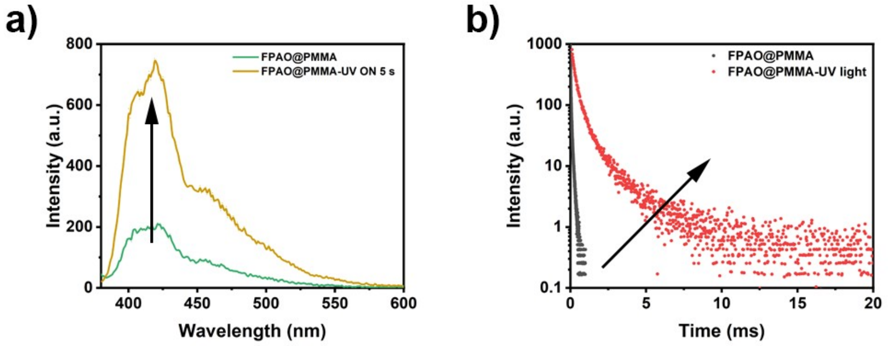

Figure S25. The a) delayed emission and b) emission decay spectra of FPAO@PMMA (0.3 wt%) with and without UV light irradiation.

3. Theoretical calculations data

Table S1

The torsion angle of XPAO in the gas phase.

Molecule	Torsion angle/°
FPAO	90.00
MOPAO	89.73
CF3PAO	89.94

Table S2

The TADF parameters of FPAO@PVA, MOPAO@PVA, and CF_3PAO@PVA.

	λ/nm	τ/ms	FWHM/nm	ΔE_{ST}/eV	PLQY/%	k_{RISC}/s^{-1}	ΔE_{ST} after protonation/eV
FPAO@PVA	433	176.9	48	0.27	34.5	5.65	0.59
MOPAO@PVA	438	295.8	55	0.26	41.4	3.38	0.66
CF3PAO@PVA	422	88.3	34	0.21	23.6	11.33	0.65

Table S3.

Singlet and triplet energy and transition configurations of XPAO in the gas phase.

Compounds	States	Energy(eV)	Transition configuration(%)
FPAO	S_1	3.54	H→L(95.7)
	T_2	3.21	H-1→L(95.0)
	T_1	2.75	H→L(96.3)
MOPAO	S_1	3.52	H→L(95.8)
	T_2	3.21	H-1→L(95.0)
	T_1	2.74	H→L(96.4)
MOPAOH$^+$	T_2	2.53	H→L(99.6)
	T_1	2.09	H-1→L(97.3)

Table S4.

Data of kinetics parameter

	τ_F/ns	Φ_{PLQY}/%	$k_{ISC}/10^8 s^{-1}$ (rough value)	k_{RISC}/s^{-1} (estimated value)
FPAO@PVA	2.55	34.5	2.57	5.65
MOPAO@PVA	1.51	41.4	3.88	3.53
CF3PAO@PVA	1.46	23.6	5.23	11.33
FPAO@PVAH$^+$	2.14	46.2	2.51	extremely slow (≈0)
MOPAO@PVAH$^+$	2.37	53.5	1.96	
CF3PAO@PVAH$^+$	1.15	6.8	8.10	

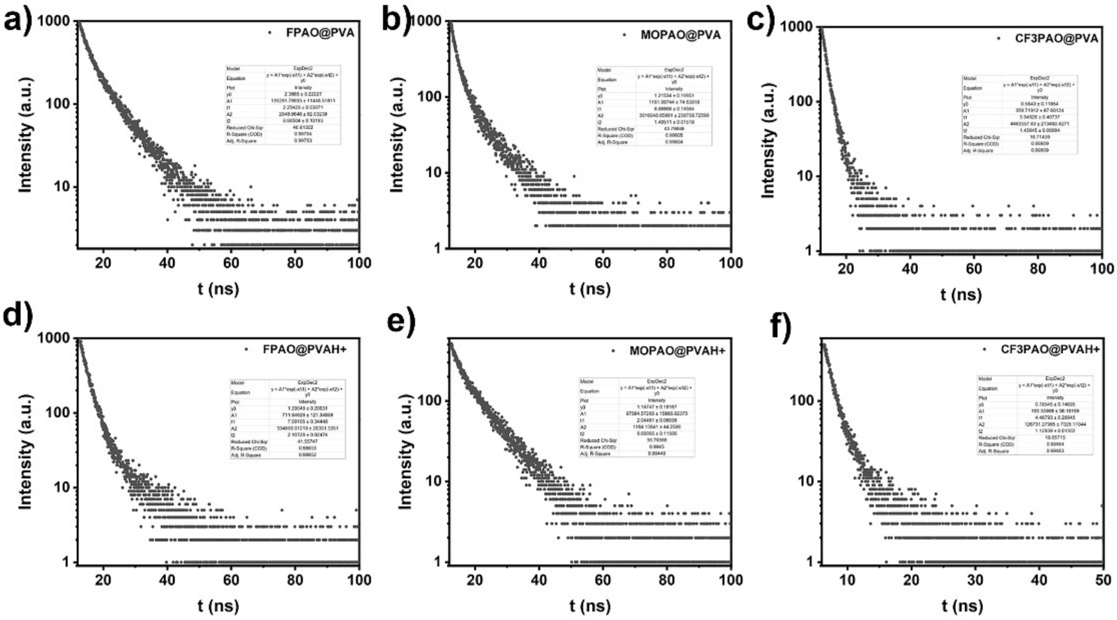

Figure S26. The fluorescence decay curve of FPAO@PVA, MOPAO@PVA, CF3PAO@PVA, FPAO@PVAH+, MOPAO@PVAH+, and CF3PAO@PVAH+.

Table S5.

HOMO-LUMO gap (eV) of XPAO (S_0, S_1, T_1) before and after protonation

	FPAO	MOPAO	CF_3PAO
S0	4.02	4.01	4.04
S1	3.75	3.73	3.40
T1	3.65	3.64	3.65
	$FPAOH^+$	$MOPAOH^+$	CF_3PAOH^+
S0	3.55	3.10	3.55
S1	3.17	2.55	3.17
T1	3.17	2.56	3.18

To elucidate the mechanism of the transition from TADF to RTP, theoretical calculations were performed on three acridone derivatives. For FPAO, the HOMO and LUMO are localized on the acridone moiety both before and after protonation, indicating localized excitation. MOPAO exhibits localized excitation before protonation but forms a D-A structure with charge transfer from the acridone to the methoxyphenyl after protonation, favoring long-wavelength emission[2] and aligning with experimental observations. CF_3PAO shows charge transfer characteristics in the S_1 state before protonation but localized excitation in other states (Table S6 and S7, ESI†).

Table S6.

HOMO and LUMO orbits of XPAO (S_0, S_1, T_1).

	FPAO	MOPAO	CF_3PAO
S0,HOMO	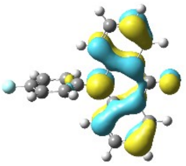	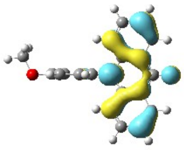	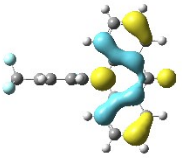
S0,LUMO	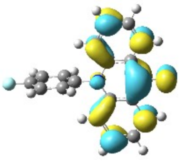	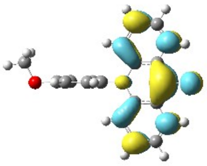	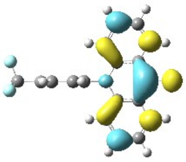
S1HOMO	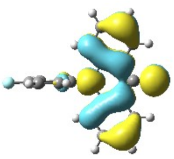	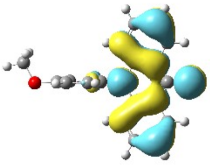	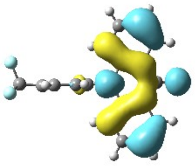
S1LUMO	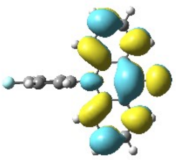	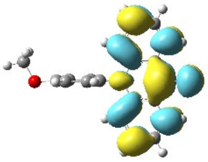	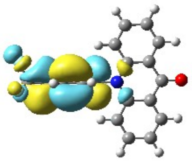
T1HOMO	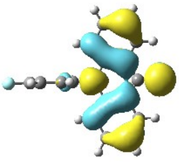	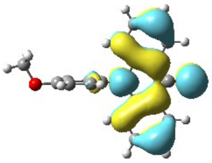	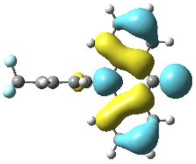
T1LUMO	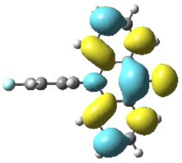	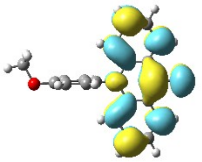	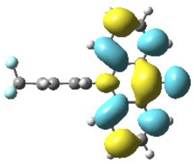

Table S7.

HOMO and LUMO orbits of XPAO after protonation (S_0, S_1, T_1).

	FPAOH$^+$	MOPAOH$^+$	CF3PAOH$^+$
S0, HOMO	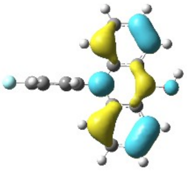	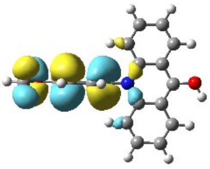	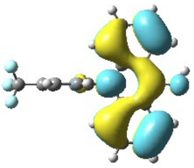
S0, LUMO	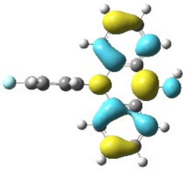	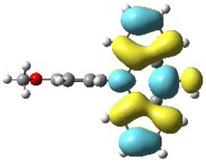	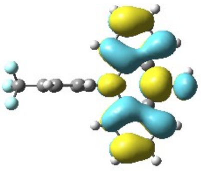
S1, HOMO	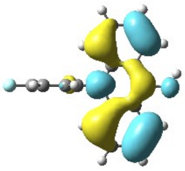	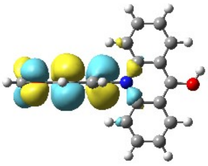	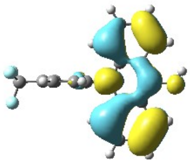
S1, LUMO	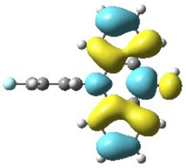	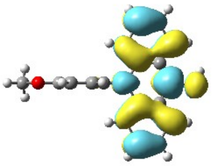	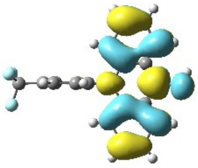
T1, HOMO	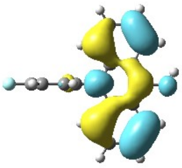	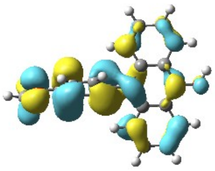	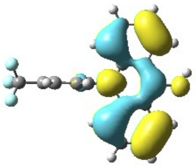
T1, LUMO	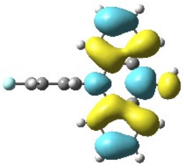	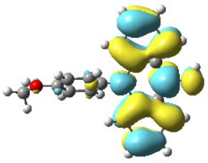	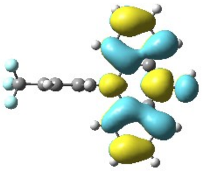

Table S8, ESI† illustrates the electrostatic potential distribution before and after protonation. Prior to protonation, the carbonyl group exhibits a high charge density, which strongly attracts protons. In contrast, after protonation, the entire molecule displays a characteristic of electron deficiency. Data of kinetics parameter is summarized in Table S9, ESI†.

Table S8.

Electrostatic potential distribution of XPAO before and after protonation.

	FPAO	MOPAO	CF3PAO
S0	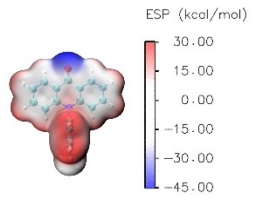	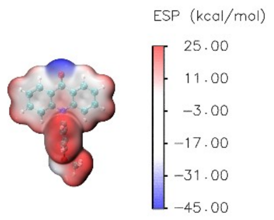	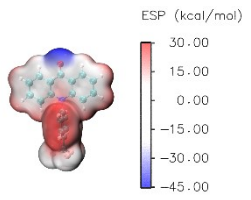
S1	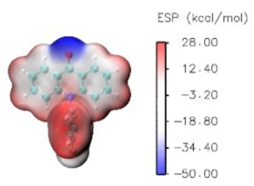	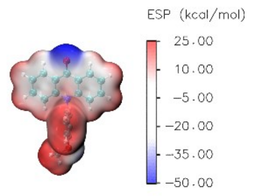	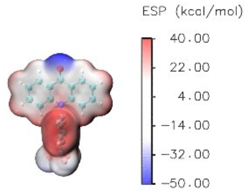
T1	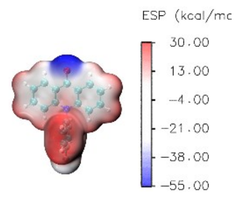	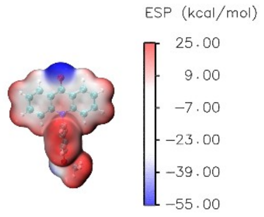	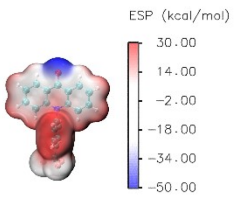
	FPAOH$^+$	MOPAOH$^+$	CF3PAOH$^+$
S0	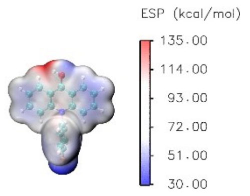	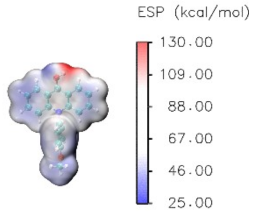	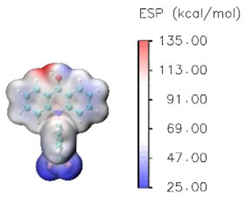
S1	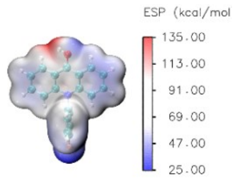	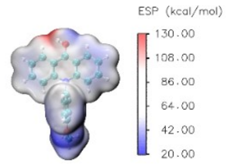	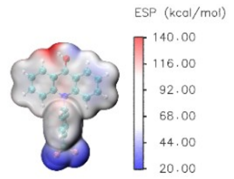
T1	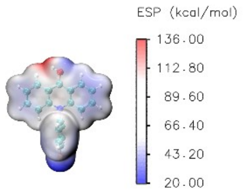	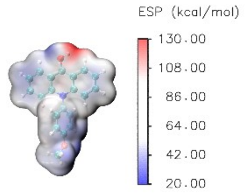	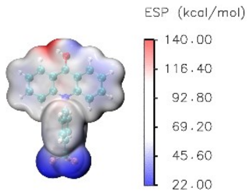

Their torsion angle doesn't show obvious change except MOPAO before and after protonation (Table S9, ESI†).

Table S9.

Torsion angle (°) of XPAO before and after protonation

	FPAO	MOPAO	CF_3PAO
S0	90.00	89.73	89.94
S1	90.00	89.73	89.48
T1	90.00	89.74	89.88
	FPAOH+	MOPAOH+	CF3PAOH+
S0	89.92	89.86	89.92
S1	89.79	89.36	89.83
T1	89.98	67.14	89.98

1. Y. Zhang, Y. Su, H. Wu, Z. Wang, C. Wang, Y. Zheng, X. Zheng, L. Gao, Q. Zhou, Y. Yang, X. Chen, C. Yang and Y. Zhao, J. Am. Chem. Soc., 2021, **143**, 13675.
2. S. Sun, L. Ma, J. Wang, X. Ma and H. Tian, Nat. Sci. Rev., 2022, **9**, nwab085.